Sugar-Induced Molten-Globule Model†

Paula R. Davis-Searles, Artemiza S. Morar, Aleister J. Saunders,‡ Dorothy A. Erie, and Gary J. Pielak*

Department of Chemistry, University of North Carolina at Chapel Hill, Chapel Hill, North Carolina 27599-3290

Received June 9, 1998; Revised Manuscript Received September 22, 1998

ABSTRACT: Proteins denature at low pH because of intramolecular electrostatic repulsions. The addition of salt partially overcomes this repulsion for some proteins, yielding a collapsed conformation called the A-state. A-states have characteristics expected for the molten globule, a notional kinetic protein folding intermediate. Here we show that the addition of neutral sugars to solutions of acid-denatured equine ferricytochrome *c* induces formation of the A-state in the absence of added salt. We characterized the structure and stability of the sugar-induced A-state with circular dichroism spectropolarimetry (CD) and NMR-monitored hydrogen−deuterium exchange experiments. We also examined the stability of the sugar-induced A-state as a function of sugar size and concentration. The results are interpreted using several models and we conclude that the stabilizing effect is consistent with increased steric repulsion between the protein and the sugar solutions.

Structural and stability studies of molten globule-like states have been instrumental in expanding our knowledge of protein folding. Molten globules, notional kinetic folding intermediates, are compact and possess nativelike secondary structure and some native tertiary contacts (*1*−*3*). An equilibrium model for the molten globule, the A-state, has been observed for several proteins, including cytochrome *c*. Adding HCl to native ferricytochrome *c* at low ionic strength denatures the protein; further addition produces the A-state (*4*). Adding salts to the acid-denatured state also leads to formation of the A-state (*5*). Circular dichroism (CD)[1] data show that the A-state possesses nativelike amounts of secondary structure (*6*) and mutagenesis studies show that it possesses some native tertiary contacts (*7*, *8*). Hydrogen−deuterium (H/D) exchange NMR studies of the NaCl-induced A-state of cytochrome *c* (*9*) show that the CD-detected secondary structure resides in native secondary structural elements (the 60s, N- and C-terminal helices).

We show that a variety of polyol osmolytes (electrically neutral, low molecular weight compounds) stabilize a low pH species with properties reminiscent of the A-state of ferricytochrome *c*. We then set out to determine if the osmolyte-induced species is structurally equivalent to the salt-induced A-state and to find the source of the sugar-induced stability.

† This work was supported by the Petroleum Research Fund administered by the American Chemical Society (28086-AC4 to G.J.P.) and the NIH (GM42501 to G.J.P. and GM54136 to D.A.E.).

* To whom correspondence should be addressed: (919) 966-3671; FAX (919) 966-3675; E-mail gary_pielak@unc.edu.

‡ Present address: Laboratory of Genetics and Aging, Department of Psychiatry, Harvard Medical School, Massachusetts General Hospital, Charlestown, MA 02129.

[1] Abbreviations: CD, circular dichroism; DQF−COSY, double-quantum filtered correlated spectroscopy; H/D exchange, hydrogen−deuterium exchange; k_{int}, first-order rate constant for peptide hydrogen−deuterium exchange; k_{obs}, observed first-order rate constant for protein hydrogen−deuterium exchange; pD, uncorrected pH meter reading; P_r, percent probability that a linear correlation coefficient arises from uncorrelated data; r, linear correlation coefficient; SASA, solvent-exposed surface area; SPT, scaled particle theory; ΔG_D, free energy of denaturation.

MATERIALS AND METHODS

Equine cytochrome *c* (Type VI, Sigma Chemical Co.) was purified by cation-exchange fast-preparative liquid chromatography, dialyzed against distilled, deionized water, and lyophilized. D_2O (99.9%) and DCl (35%) were from Cambridge Isotope Laboratories, Inc. Prior to the NMR experiments, melezitose was dissolved in D_2O and lyophilized to exchange labile protons for deuterons.

Circular Dichroism. CD spectra were acquired at 1 °C on an Aviv 62DS spectropolarimeter equipped with a temperature-controlled five-position sample changer. The cytochrome *c* concentration was 15 μM for far-UV spectra and 50 μM for near-UV/Soret spectra. Native-state spectra were acquired in 50 mM sodium acetate, pH 4.6. Other spectra were acquired in a pH 2.0 HCl solution containing either 2.0 M NaCl or 0.7 M melezitose. Each scan was acquired with 0.5 nm resolution and an averaging time of 3 s/point in a 0.1 cm cuvette. Each spectrum is the average of three scans.

Isothermal Titrations. Data were acquired in pH 2.0 HCl at 1 °C. Samples were preincubated for 10 min at 1 °C before data acquisition. Glycerol, glucose, and galactose titrations were performed by acquiring spectra for individual samples. Sucrose, trehalose, melezitose, and stachyose titrations were performed by monitoring the ellipticity at 222 nm over 1 min and averaging the results. The fraction denatured, α, was calculated by using the minimum ellipticity at 222 nm of the folded baseline to represent the fully formed A-state. The sigmoidal curves are analogous to those from thermal or chemical denaturations (*10*) except that we observe folding as a function of increased osmolyte concentration. Using data from the transition region, we plotted $-\ln K_D$ as a function of osmolyte concentration [where $K = \alpha/(1 - \alpha)$] and calculated the slope and intercept. To replicate the conditions of the NMR experiment (see below), the melezitose titration was repeated in D_2O solution with a fully D_2O-exchanged sample at 20 °C. Error estimates were determined by incorporating the fitting uncertainties into a linear model.

10.1021/bi981364v CCC: $15.00
Published on Web 11/12/1998

Table 1: Dependence of $\Delta\Delta G_D$ on Osmolyte Concentration, $\delta\Delta\Delta G_D/\delta C_{os}$, for the A ⇄ D Transition, pH 2, 1 °C[a]

			$\delta\Delta\Delta G_D/\delta C_{os}$ [kcal/(mol·M)]			
				calculated		
osmolyte	radius (Å)	type	observed	excluded volume	SPT sphere	SPT kissing spheres
glycerol	2.7	half saccharide	0.7 ± 0.1	9.3−19.6	0.4−0.8	1.2
glucose	3.2	monosaccharide	1.8 ± 0.3	9.6−20.4	0.6−1.2	2.2
galactose		monosaccharide	1.5 ± 0.2			
sucrose	4.0	disaccharide	2.2 ± 0.1	10.1−21.4	1.0−2.0	3.8
trehalose		disaccharide	2.4 ± 0.1			
melezitose	4.6	trisaccharide	4.1 ± 0.3	10.4−22.1	1.2−2.4	5.0
stachyose	5.0	tetrasaccharide	5.1 ± 0.2	10.7−22.6	1.4−2.8	5.9

[a] Excluded-volume theory (*38*) and scaled particle theory (*19*) were used to obtain the calculated values as described in the text.

NMR-Monitored Hydrogen−Deuterium Exchange. Six milliliters of ~6 mM ferricytochrome *c* was prepared in 0.7 M melezitose and the pH was adjusted to 2.0 with HCl. After 12 0.5-mL samples were aliquotted, each sample was exchanged into the equivalent D_2O solution at pD 2.0 by using a preequilibrated NAP-5 G-25 gel-filtration column (Pharmacia). A 1.0 mL fraction containing the protein was collected (pD 2.3). The exchange reaction was considered to have started upon elution of the first drop of red solution. The samples were incubated at 20 °C for log-spaced time intervals from 10 min to 3 weeks. Exchange was stopped by passing each 1.0 mL sample over a PD-10 G-25 gel-filtration column (Pharmacia), which was equilibrated and eluted with degassed 50 mM sodium phosphate buffer in D_2O, pD 5.8 (quench buffer). The first 2.0 mL of red eluent was collected. The next 0.5 mL was collected in a separate vessel as it contained ~14 mM melezitose. The cytochrome *c* in the eluents was immediately reduced with $Na_2S_2O_4$ in D_2O (40 mM final concentration) and chilled on ice. The melezitose-containing fraction was diluted 4-fold with quench buffer. After each portion was concentrated with a Centricon-3 concentrator (Amicon), the two portions were pooled, sodium ascorbate in D_2O was added to a final concentration of 4 mM, and 1,4-dioxane was added to a final concentration of 1.2 mM. The final uncorrected pH meter reading (pD) was 4.7, and the final protein concentration was 3.0−3.5 mM. Samples were sealed under Ar and stored at 4 °C until NMR spectra were acquired. To generate a time 0 sample, lyophilized protein was dissolved in quench buffer and reduced, the pD was adjusted to 4.7, and the NMR data were immediately collected.

The NaCl experiment was the same as that described above except for the quench step. The quench was performed with NAP-5 columns (after the A-state samples were concentrated to 0.5 mL) preequilibrated with 50 mM sodium phosphate buffer in D_2O, pD 5.3, and 20 mM sodium ascorbate. The final pD was 5.0. Samples were sealed under N_2 and stored at 4 °C.

NMR Spectroscopy. One-dimensional ^1H and 2D gradient-enhanced DQF−COSY spectra were collected on a Bruker AMX500 spectrometer at 25 °C in the phase-sensitive mode using time-proportional phase incrementation (*11*) in both dimensions. The residual HOD resonance was suppressed by presaturation. The spectral width was 9090.9 Hz. Spectra were referenced relative to internal 1,4-dioxane (3.741 ppm). The t_2 dimension comprised 40 repetitions of 1024 complex points and the t_1 dimension comprised 512 increments for a total acquisition time of 12 h per sample. Data were processed on a personal computer with NUTS-2D version 5.105 software (Acorn NMR, Inc., Fremont, CA). Prior to Fourier transformation, the data were resolution-enhanced with a 30°-shifted sine-squared function (*12*). The data were zero-filled in both dimensions to yield a 2048 × 2048 matrix of real points. The NH−Cα cross-peak assignments of Wand et al. (*13*) were used to analyze the data. After an absolute value calculation was performed, cross-peak volumes were measured relative to that of the Thr63$\beta\gamma$ cross-peak. The volumes of overlapping cross-peaks were dissected by using a slice-addition method. The first-order rate constant for exchange, k_{obs}, was determined by fitting these data to the function volume $= A + B[\exp(-k_{obs}t)]$ by using SigmaPlot 3.06 (Jandel Corp.).

Calculation of Radii and Implementation of Scaled Particle Theory. Hard-sphere radii of 1.4, 2.5, 3.2, 4.0, 4.6, and 5.0 Å for water, glycerol, monosaccharides, disaccharides, trisaccharides, and tetrasaccharides were calculated as described by Edward (*14*). The solvent-accessible surface area (SASA) of fully unfolded cytochrome *c*, 1.8×10^4 Å^2, was estimated by using the equation of Richards (*15*):

$$SA = (1.45 \times 10^{-16})N_A \text{ cm}^2/\text{g}$$

and a molecular weight of 12.6×10^4 g/mol. Chalikian et al. (*16*) estimate that the A-state exposes 60% of the SASA of fully unfolded cytochrome *c*. For a spherical model, this gives an A-state radius of 30 Å. Chalikian et al. also estimate that the acid-denatured state exposes between 70% and 80% of the SASA of the fully unfolded protein. For a spherical model, this gives a radius for the acid-denatured protein of between 32 and 34 Å. Using the SASA of the native state (*17*), 6115 Å^2, and the SASA for the acid-denatured state, we predict a 2.1−2.4-fold increase in SASA upon acid denaturation of the native state. This range is consistent with the idea that native proteins expose between 2 and 3 times the SASA of the native state upon denaturation (*18*). We used the SPT described by Berg (*19*) with the radii given above. Specifically, we used equations A1, A4, A5, and A9 in Berg's paper for the spherical model. Equation A11 was used for the kissing-sphere model.

RESULTS

CD Spectra of Salt- and Sugar-Induced A-States. Adding any of the polyol osmolytes listed in Table 1 to acid-denatured cytochrome *c* gives a spectrum resembling that of the A-state formed in 2.0 M NaCl, pH 2.0. Figure 1A shows the far-UV spectra of the denatured state, the native state, the salt-induced A-state, and the melezitose-induced

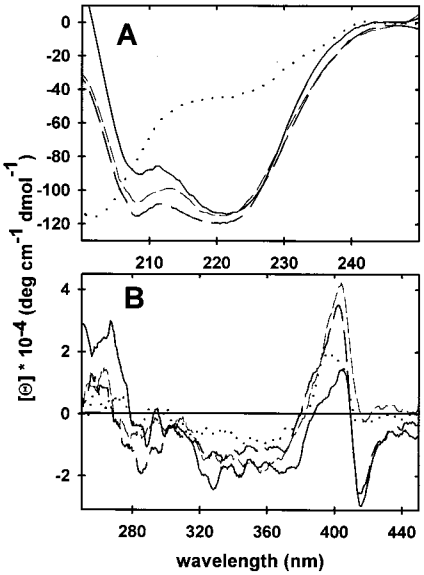

FIGURE 1: Far-UV (A) and near-UV/Soret CD spectra (B) at 20 °C of the denatured state at pH 2.0 (dotted curve), the native state at pH 4.6 in 50 mM sodium acetate (solid curve), and the A-states formed in 2.0 M NaCl at pH 2.0 (thin dashed curve) and 0.7 M melezitose at pH 2.0 (thick dashed curve).

species. The native-state far-UV spectra possess the characteristic helix minima at 208 and 222 nm and the sizes of the minima are consistent with the amount of α-helix observed in the crystal structure (*20*). The species induced by NaCl or melezitose (Figure 1), and by all the other osmolytes listed in Table 1, exhibit far-UV spectra closely resembling that of the native state, indicating that they all have nativelike amounts of secondary structure. As shown in Figure 1B, neither salt nor melezitose produces the native near-UV and visible CD spectra. In fact, none of the osmolytes, nor combinations of osmolytes and salt, at any concentration, induces native near-UV or visible spectra. Interestingly, sugars, but not salt, induce the negative Soret Cotton effect at 415 nm of the native protein. This observation suggests that the heme environment near phenylalanine 82 (*21*) is more nativelike in sugar than in salt. In summary, the additives cannot refold acid-denatured cytochrome *c* to its native state but rather stabilize a low-pH species having nativelike amounts of secondary structure and some nonnative tertiary structure.

NMR-Detected Hydrogen−Deuterium Exchange. We used the method pioneered by Hughson et al. (*22*) and Jeng et al. (*9*) in which a quench step "traps" the partially exchanged intermediates in the more stable native state, facilitating NMR-based exchange rate measurements. These NMR-detected H/D exchange experiments comprise three steps: initiation, exchange, and quench. The experiment is initiated by transferring the aqueous cytochrome *c* (pH 2.0) containing NaCl or melezitose to the equivalent D_2O solution. Twelve samples were incubated at 20 °C to allow labile protons to exchange with solvent deuterons. After various times, the samples are quenched in a rapid two-step process. First, the pD was raised to ∼5 to induce formation of the native state. Second, the heme-bound iron was reduced from Fe^{3+} to Fe^{2+} with $Na_2S_2O_4$, further slowing exchange (*23*−*25*). To preserve the reduced protein, we exchanged the samples into degassed quench buffer and sealed them under Ar or N_2.

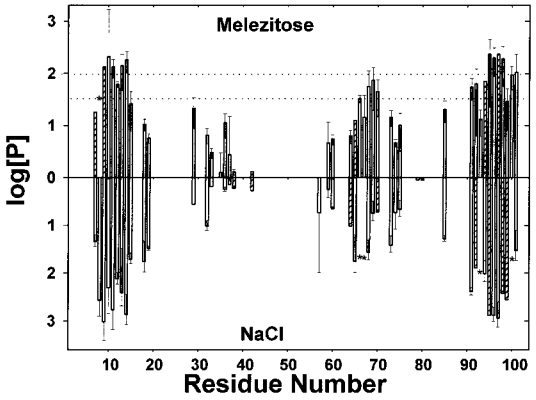

FIGURE 2: Histograms of log *P* versus residue number for the A-state formed in 1.5 M NaCl, pD 2.4 (lower panel), and 0.7 M melezitose, pD 2.3 (upper panel). Error bars represent the standard deviation of the fit. Hatched bars indicate estimates for very slow- or very fast-exchanging amide protons; asterisks indicate the cross-peak was missing or obscured. The horizontal dashed lines represent the upper and lower limits of log P calculated from titration data at 20 °C.

The first-order rate constants for exchange, k_{obs}, were calculated as described in Materials and Methods. The first-order rate constants for intrinsic exchange, k_{int}, were calculated with the program SPHERE (*26*−*30*). We then calculated a protection factor, P ($= k_{int}/k_{obs}$), for each measured amide proton. Usually, large P values indicate involvement of the amide proton in a H-bond (*9*).

First, we reproduced the NaCl experiment (Figure 2, lower panel) (*9*). We then repeated the experiment with 0.7 M melezitose in the absence of added salt (Figure 2, top panel). Like the NaCl data, amide protons in the major units of native secondary structure, the 60s-, N-terminal, and C-terminal helices, are all protected in the sugar-induced state. This observation indicates that the secondary structure observed by CD is native secondary structure. The quantitative agreement between log *P* values shows that the stability of this structure is the same for the sugar- and salt-induced states. However, the stability of these structures in the A-states and the native state are different; the log *P* values are between 1 and 3 for the A-state (Fe^{3+}) and between 4 and 8 for the native state (Fe^{3+}) (*9*, *23*, *31*). This comparison shows that the A-states possess some nonnative tertiary structure, consistent with the conclusion derived from examination of the near-UV/Soret CD spectra (Figure 1B). This is not to say that all native tertiary structure is absent. For instance, Ile 85 and Leu 68 are both well protected, probably because they form a tertiary H-bond in the hydrophobic core. Nevertheless, H-bonds from native loops and turns are poorly protected in the A-state, implying that the tertiary structure is flexible. In summary, the observation of nativelike secondary structure and the presence of nonnative tertiary structure and certain native tertiary contacts is consistent with the molten globule hypothesis.

Stability of the Sugar-Induced Species. We examined the effect of sugar concentration and size on the free energy of denaturation (ΔG_D). The isothermal titrations of these sugars into acid-denatured cytochrome *c* yield reversible sigmoidal curves. Each curve was analyzed by using a two-state model and the results are shown in Figure 3. As shown in Figure 4, plots of $\Delta\Delta G_{obs}$ (ΔG_D for denaturation of the A-state in osmolyte solution minus the extrapolated ΔG_D in buffer

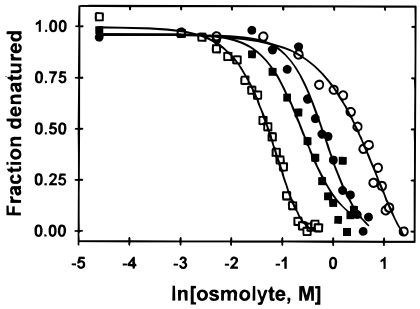

FIGURE 3: Plots of fraction denatured versus the natural logarithm of osmolyte concentration for stachyose (□), melezitose (■), trehalose (●), and glycerol (○).

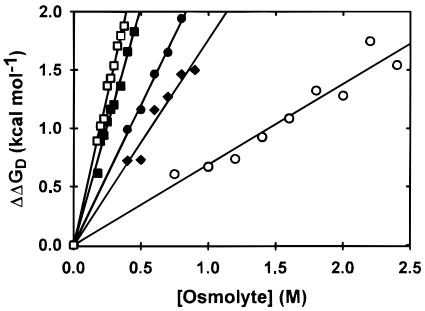

FIGURE 4: Plots of $\Delta\Delta G_D$ versus osmolyte concentration for stachyose (□), melezitose (■), trehalose (●), glucose (◆), and glycerol (○).

alone) versus sugar concentration are linear. The data for every sugar listed in Table 1 give a correlation coefficient (r) of ≥ 0.994 and a percent probability that r arises from uncorrelated data (P_r) of $<0.5\%$. The slopes, $\delta\Delta\Delta G_{obs}/\delta C_{os}$, for all the sugars studied are given in Table 1. To compare the NMR data to the isothermal denaturation data, we also studied the effect of melezitose in D_2O using fully exchanged samples. The resulting ΔG_D is 2.3 ± 0.3 kcal/mol at 0.7 M melezitose and 20 °C.

Comparison of Local and Global Stabilities. The horizontal dashed lines in Figure 2 represent the upper and lower limits of log P derived from isothermal CD-detected experiments ($\Delta G_D = -2.3RT \log P$). Comparison of log P for the most well-protected amide protons to the range of global stabilities suggests that the most well-protected amide protons in the melezitose-induced A-state are exposed only upon complete unfolding. For some amide protons, however, the maximum local-unfolding free energy exceeds the global-denaturation free energy. Such superprotection (*32*) has been observed for several proteins. It has been suggested that superprotection arises from proline isomerization (*33*) and latent structure in the maximally unfolded state populated under the native conditions used for NMR (*34*).

DISCUSSION

We have shown that the A-state can be formed from the acid-denatured state in the *absence* of added salt. The osmolyte-induced A-state has the same native secondary structure and many of the same native tertiary contacts found in the salt-induced species. We also examined the effect of osmolyte size and concentration on the stability of the sugar-induced A-state. At fixed osmolyte concentration, $\Delta\Delta G_D$ increases with osmolyte size and is linearly related to osmolyte concentration (Figure 4). As shown in Table 1, the slope, $\delta\Delta\Delta G_D/\delta C_{os}$, also increases with osmolyte size.

What is responsible for A-state formation in osmolyte solution? Several analyses are currently used to interpret the effect of additives on protein stability. Osmotic stress analysis (*35*) quantifies the effect in terms of the number of water molecules bound to the end states, in this case the A-state and the acid-denatured state. For our data, this analysis gives the unrealistic conclusion that the number of water molecules released on folding varies with the identity of the sugar. Most importantly, however, this analysis has been shown to be theoretically unsound (*36*).

Bolen and colleagues (*37*) use apparent water-to-osmolyte-solution transfer free energies for side-chain and backbone models to interpret the increase in stability. They conclude that unfavorable interactions between the fully unfolded protein and the osmolyte solution drive folding. That is, the decreased exposure of the backbone on folding is the major driving force for osmolyte-induced stabilization. Our sucrose data are consistent with this idea, but a more complete analysis is not possible because the transfer free energy for heme is unavailable. Also, analysis of the size effect must await the determination of transfer free energies in other polyol osmolyte solutions. Finally, the assumption that the denatured state is fully unfolded merits examination in the light of the idea that denatured states do not expose all their potential SASA (*18*).

Winzor's analysis (*38*) focuses on the nonideality of osmolyte solutions caused by excluded volume effects. Data are interpreted by using the following relationship:

$$\frac{\delta\Delta\Delta G_D}{\delta C_{os}} = -RT(U_A - U_D)$$

where U_A and U_D are the covolumes of the A-state and the acid-denatured state, respectively, and C_{OS} is the molar osmolyte concentration. The covolumes are given by

$$U = {}^4/_3\pi N(r_i + r_m)^3$$

where N is Avogadro's number, r_i is the radius of the state, and r_M is the radius of the osmolyte. Since a range of estimated radii for the acid-denatured state is available (see Materials and Methods), we calculated upper and lower estimates of $\delta\Delta\Delta G_D/\delta C_{os}$ for each osmolyte (half-saccharide, monosaccharide, *etc*.) As shown in Table 1, this analysis accounts for the increase with both concentration and size of osmolyte but overestimates the size of the effect, sometimes by more than a factor of 25. A large mismatch has also been observed for the thermal denaturation of RNase in glycerol (*38*). The reason for the mismatch is unclear, but it is interesting to note that the mismatch decreases as the size of the osmolyte increases.

Timasheff interprets the effect of additives in terms of preferential hydration of the protein surface (*39*, *40*). Sugars belong to a class of additives that do not interact chemically with the protein surface. In this case, preferential hydration is related to the increase in air−water surface tension upon addition of the additive. Kaushik and Bhat (*41*) also show that the ability of polyol osmolytes to increase protein stability is related to their ability to increase surface tension. The idea is that as the surface tension increases, more work is required to create a cavity of a given surface area in the solvent, thereby favoring states with smaller surface areas

over states with larger surface areas. Unfortunately, air−water surface tensions cannot be used to *quantify* the effect of sugars on protein stability because surface tension does not coincide with the interfacial tension between the protein and the solvent (*42*). That is, there is no vapor in the cavity—it is filled with protein—and air is probably not a good model for a protein surface.

We find that scaled particle theory (SPT) (*43*) provides the best framework for quantifying our results. SPT treats all the solution components as hard spheres and predicts the free energy required for producing a cavity of a given surface area in the solvent when the only interactions are steric repulsions between the spheres (*42*). In this treatment, increasing the osmolyte concentration and/or size results in an increase in the steric repulsion between the species in solution. Therefore, the free energy for forming a cavity in osmolyte solution will increase relative to the free energy for forming the same sized cavity in pure solvent. Since the free energy of cavity formation increases with cavity size (*42*), species with smaller surface areas (the A-state) are favored over species with larger surface areas (the acid-denatured state).

Minton (*44*) and colleagues have pioneered the use of SPT to explain the effects of macromolecules on protein association. We used Berg's implementation of SPT (*19*) because it considers both the solvent and the solute and because the protein can be treated as either a sphere or a dumbbell. Since a range of estimated radii for the acid-denatured state is available (see Materials and Methods), we calculated upper and lower estimates of $\delta\Delta\Delta G_D/\delta C_{os}$ for each osmolyte (half saccharide, monosaccharide, etc.). $\delta\Delta\Delta G_D/\delta C_{os}$ was calculated over the osmolyte concentration ranges used in the experiments (approximately the limit of solubility). Although the calculated functions are curved, they approximate a line ($r > 0.99$, $P_r < 0.5\%$) over the concentration ranges used. The results are shown in Table 1. The spherical model generally underestimates the slopes but never by more than a factor of 4. The similarity between the calculated and observed slopes suggests that the increase in steric repulsions with increasing osmolyte size and concentration explains the stabilizing effect.

We also examined the effect of shape by using a dumbbell model for the acid-denatured state (*19*). The A-state was treated as a sphere, but the denatured state was modeled as a dumbbell of kissing spheres with the same volume as the A-state. As described above, the calculated functions can be treated as straight lines. For this model, the agreement between the observed and calculated slopes is nearly quantitative (Table 1); the model overestimates the slopes but never by more than a factor of 1.7. This result suggests that surface area, not volume, is the controlling feature. We conclude that steric repulsions are the major driving force of A-state formation in solutions of polyol osmolytes. Identical results have been obtained for the sugar-induced A-state of yeast ferricytochrome *c*. These results, other results describing the effect of osmolytes on the thermal denaturation of native yeast ferricytochrome *c*, and a more complete discussion of the thermodynamics will be published separately (Aleister J. Saunders, Paula R. Davis-Searles, Devon L. Allen, Gary J. Pielak, and Dorothy A. Erie, submitted for publication).

Salt Is Different. Goto et al. (*6*) suggest that anion binding causes the acid-denatured state to condense to the A-state. A comparison of our data to those of Goto et al. shows that the salt-induced effect is stronger than the sugar-induced effect; the observed slopes (Table 1) range from 0.7 to 5.1 kcal/(mol·M), but for salts the slopes are 10^4 times greater. In other words, 0.1−2.0 M sugar induces formation of the A-state, but salts are effective in the micromolar to millimolar range (*6*). Goto et al. show that anion charge is the main determinant of salt effectiveness (more highly charged species are more effective), although there is a small size dependence. Specifically, I^- (2.1 Å radius) is more effective than Cl^- (1.7 Å) and concentrations required to fold half the protein molecules at 20 °C are 13 and 48 mM, respectively. In addition, SPT calculations suggest that steric repulsions do not explain the ability of salts to induce A-state formation. Use of anion radii given above yields a slope that is much too small, while use of SPT and the observed slope [10^4 kcal/(mol·M)] gives an unrealistically large anion radius.

Conclusions. We have shown that the addition of sugars to acid-denatured cytochrome *c* gives a species that is nearly identical to the A-state formed by addition of salt. The fact that the stabilizing effect increases with both the size and the concentration of the sugars and the success in using SPT to explain the data suggests that increases in steric repulsion drive A-state formation in osmolyte solutions. The results also show that sugars and salts act by different mechanisms. Anions bind more tightly to the more densely charged species, the A-state. On the other hand, sugars increase the steric repulsion between solution components, favoring the smaller A-state over the larger acid-denatured state.

NOTE ADDED IN PROOF

Recently, Qu et al. (*45*) have reported that osmolytes drive compaction of an otherwise unfolded protein.

ACKNOWLEDGMENT

We thank Gregory B. Young for assistance with NMR and the Pielak group for comments on the manuscript.

REFERENCES

1. Ptitsyn, O. B. (1987) *J. Protein Chem. 6*, 273−293.
2. Kuwajima, K. (1989) *Proteins*: *Struct., Funct., Genet. 6*, 87−103.
3. Roder, H., and Colon, W. (1997) *Curr. Opin. Struct. Biol. 7*, 15−28.
4. Goto, Y., Calciano, L. J., and Fink, A. L. (1990) *Proc. Natl. Acad. Sci. U.S.A. 87*, 573−577.
5. Ohgushi, M., and Wada, A. (1983) *FEBS Lett. 164*, 21−24.
6. Goto, Y., Takahashi, N., and Fink, A. L. (1990) *Biochemistry 29*, 3480−3488.
7. Marmorino, J. L., and Pielak, G. J. (1995) *Biochemistry 34*, 3140−3143.
8. Marmorino, J. L., Lehti, M., and Pielak, G. J. (1998) *J. Mol. Biol. 275*, 379−388.
9. Jeng, M. F., Englander, S. W., Elöve, G. A., Wand, A. J., and Roder, H. (1990) *Biochemistry 29*, 10433−10437.
10. Pace, C. N., Shirley, B. A., and Thomson, J. A. (1989) in *Protein Structure*: *A Practical Approach* (Creighton, T. E., Ed.) pp 311−330, IRL Press at Oxford University Press, Oxford, England.
11. Marion, D., and Wüthrich, K. (1983) *Biochem. Biophys. Res. Commun. 113*, 967−974.

12. Cavanagh, J., Fairbrother, W. J., Palmer, A. G., III, and Skelton, N. J. (1996) *Experimental ^{1}H NMR Methods*: *Principles and Practice*, Academic Press, New York.
13. Wand, A. J., Di Stefano, D. L., Feng, Y. Q., Roder, H., and Englander, S. W. (1989) *Biochemistry 28*, 186−194.
14. Edward, J. T. (1970) *J. Chem. Educ. 47*, 261−270.
15. Richards, F. M. (1977) *Annu. Rev. Biophys. Bioeng. 6*, 151−176.
16. Chalikian, T. V., Gindikin, V. S., and Breslauer, K. J. (1995) *J. Mol. Biol. 250*, 291−306.
17. Chalikian, T. V., Totrov, M., Abagyan, R., and Breslauer, K. J. (1996) *J. Mol. Biol. 260*, 588−603.
18. Creamer, T. P., Srinivasan, R., and Rose, G. D. (1997) *Biochemistry 36*, 2832−2835.
19. Berg, O. (1990) *Biopolymers 30*, 1027−1037.
20. Berghuis, A. M., and Brayer, G. D. (1992) *J. Mol. Biol. 223*, 959−976.
21. Pielak, G. J., Oikawa, K., Mauk, A. G., Smith, M., and Kay, C. M. (1986) *J. Am. Chem. Soc. 108*, 2724−2727.
22. Hughson, F. M., Wright, P. E., and Baldwin, R. L. (1998) *Science 249*, 1544−1548.
23. Marmorino, J. L., Auld, D. S., Betz, S. F., Doyle, D. F., Young, G. B., and Pielak, G. J. (1993) *Protein Sci. 2*, 1966−1974.
24. Cohen, D. S., and Pielak, G. J. (1995) *J. Am. Chem. Soc. 117*, 1675−1677.
25. Pascher, T., Chesick, J. P., Winkler, J. R., and Gray, H. B. (1996) *Science 271*, 1558−1560.
26. Molday, R. S., Englander, S. W., and Kallen, R. G. (1972) *Biochemistry 11*, 150−158.
27. Bai, Y., Milne, J. S., Mayne, L., and Englander, S. W. (1993) *Proteins*: *Struct., Funct., Genet. 17*, 75−86.
28. Connelly, G. P., Bai, Y., Jeng, M. F., and Englander, S. (1993) *Proteins*: *Struct., Funct., Genet. 17*, 87−92.
29. Zhang, Y.-Z. (1995) Doctoral Dissertation, University of Pennsylvania, Philadelphia, PA.
30. Zhang, Y.-Z. and Sauder, M. Web site http://www.fccc.edu/research/labs/roder/.
31. Milne, J. S., Mayne, L., Roder, H., Wand, A. J., and Englander, S. W. (1998) *Protein Sci. 7*, 739−745.
32. Betz, S. F., Marmorino, J. L., Saunders, A. J., Doyle, D. F., Young, G. B., and Pielak, G. J. (1996) *Biochemistry 35*, 7422−7428.
33. Bai, Y., Milne, J. S., Mayne, L., and Englander, S. W. (1994) *Proteins*: *Struct., Funct., Genet. 20*, 4−14.
34. Clarke, J., and Itzhaki, L. S. (1998) *Curr. Opin. Struct. Biol. 8*, 112−118.
35. Parsegian, V. A., Rand, R. P., and Rau, D. C. (1995) *Methods Enzymol. 259*, 43−94.
36. Timasheff, S. N. (1998) *Proc. Natl. Acad. Sci. U.S.A. 95*, 7367.
37. Liu, Y., and Bolen, D. W. (1995) *Biochemistry 34*, 12884−12891.
38. Shearwin, K. E., and Winzor, D. J. (1990) *Arch. Biochem. Biophys. 282*, 297−301.
39. Lin, T. Y., and Timasheff, S. N. (1996) *Protein Sci. 5*, 372−381.
40. Timasheff, S. N. (1993) *Annu. Rev. Biophys. Biomol. Struct. 22*, 67−97.
41. Kaushik, J. K., and Bhat, R. (1998) *J. Phys. Chem. 102*, 7058−7066.
42. Reiss, H. (1966) *Adv. Chem. Phys. 9*, 1−84.
43. Reiss, H., Frisch, H. L., and Lebowitz, J. L. (1959) *J. Chem. Phys. 31*, 369−380.
44. Minton, A. P. (1993) *J. Mol. Recognit. 6*, 211−214.
45. Qu, Y., Bolen, C. L., and Bolen, D. W. (1998) *Proc. Natl. Acad. Sci. U.S.A. 95*, 9268−9273.

BI981364V